ET Enterprises electron tubes

technical reprint

R/P100

photomultiplier dark current induced by the natural and cosmic ray background

photomultiplier dark current induced by the natural and cosmic ray background

A G Wright, Electron Tubes Ltd,
Bury Street,
Ruislip, Middx, HA4 7TA, UK

technical reprint RP/100

1 introduction

A technical paper with the title 'Cosmic ray induced dark current in photomultipliers' was published by A T Young some 40 years ago [1]. The author observed that most of the dark current disappeared upon cooling of a photomultiplier. However, that which remained contained large bursts, the origin of which had up to that time not been explained. Using no more than an oscilloscope and a strip chart recorder, Young was able to account for the noisy component of the background in terms of the known muon rate of ~1 per cm per minute [2], [3] (see **table 1**). In today's industrial and scientific equipment, the chart recorder has been replaced by a PC with an ADC card programmed to take a dc reading several times per second, or as required. Some users are puzzled by the appearance of spikes in the background, which annoyingly persist, despite attempts to filter them by changing the bandwidth or by changing the photomultiplier. All too often the photomultiplier is 'blamed' and branded 'unstable'. Of course, this may be true: the spikes may arise from poor housing design or from photomultiplier breakdown or a combination of both – but that is a different topic.

Photomultiplier dark current is the integral of the dark count spectrum suitably waited by pulse height, plus the leakage current. Any attempt to explain the noisy background must start from knowing the spectrum of the dark counts. The essence of the present work lies in measuring and accounting for the pulse height distribution of dark counts in a range of photomultiplier sizes – from 38 to 134 mm in diameter. This information is used to explain the background effects seen in electrometer type measurements made at low light levels. In addition, spectral information on the dark counts is of direct relevance to those measuring pulse height distributions in scintillation spectroscopy, for example. High energy events seen in the background spectrum of a NaI(Tl) scintillation assembly, also originate from the cosmic ray background and quantitative information on this application will also be provided.

2 the nature of the cosmic ray background

Cosmic ray research has a history dating back to 1912 when Hess established the nature of this radiation using balloon-borne detectors. The composition of the background, with the relative proportions, is given in Table 1. The highly energetic primaries produce showers which contain many secondary particles spread over square kilometres of the earth's surface. What we observe at ground level is a mixture of particles created in the atmosphere following the initial interaction of the primary high energy gammas, neutrinos, protons, alpha particles and light nuclei, some of which have energy approaching 10^{21} eV. (note a typical gamma ray produced by radio-active decay is ~10^{6} eV. The precise composition and rate of events at any one location on earth depends on latitude and altitude, but for our purposes the cosmic ray background is essentially constant over time and with location.

The flux at sea-level is classified in terms of a soft component and a hard component – the latter being muons. The soft component as the name implies is easily absorbed by an overburden of about 10 metres. At depths beyond this, the composition is primarily muons and their daughter products. In order to escape the muon background it is necessary to operate at very great depths underground. The current, massive, astrophysics and other low background experiments searching for ultra-high energy neutrino events and dark matter, are located at depths of a mile or so underground. But,

even at these depths, the occasional muon will still be observed.

Table 1 The composition of the cosmic ray flux at sea-level, [3]

Total	3×10^{-2} $s^{-1}cm^{-2}$
muons	63%
neutrons	21%
electrons	15%
protons/pions	<1%

The muon angular distribution varies as $\cos^2\theta$

3 other sources of photomultiplier background

There are many studies in the literature on this topic and only a brief resume will be given here. The reader is referred to other papers by Young [4] and by the author [5]. The latter may be conveniently down-loaded from our website (www.electrontubes.com). For present purposes we divide photomultiplier background into 4 distinct regions of interest.

A – less than ½ photoelectron equivalent. A portion of this is statistically under-amplified single photoelectron events and the remainder is dark count originating from the dynodes of the multiplier.

B – between ½ and 2 photoelectrons equivalent. Counts in this part of the spectrum originate from the photocathode. Some are of thermal origin whilst others derive from photon feedback.

C – these range from 2 to about 10 photoelectrons. They are attributed to ion pulses, afterpulses and natural radiation in the glass of the pmt and from the environment.

D – greater than 10 photoelectrons equivalent. This is the region of particular interest in this study which includes contributions from the soft and hard components of the cosmic ray background.

Natural radioactivity makes a significant contribution to C from the well-known sources: ^{40}K, ^{232}Th and ^{238}U. The presence of these isotopes is established by the appearance of characteristic peaks in the NaI(Tl) energy spectrum (see **figure 7(b)** and [4], also available from the web).

4 observations with an oscilloscope

There is much to be learned from looking at the output signal from a photomultiplier on a fast oscilloscope. Sub- and single-photoelectron signals of type A and B can be observed by setting the gain of the photomultiplier to about 5×10^6 and the oscilloscope sensitivity in the region of 5 to 20 mV/cm (select 50 Ω input impedance). The trigger rate will lie in the range of 20 to 1000 per second, depending on the particular tube selected, and confirming the contribution from sources A and B. Upon reducing the gain of the photomultiplier by a factor of 10, the rate will drop substantially as only contributions from C and D now trigger.

A photomultiplier, of small diameter and fabricated with a thin window, produced a trace similar to that shown in **figure 1**.

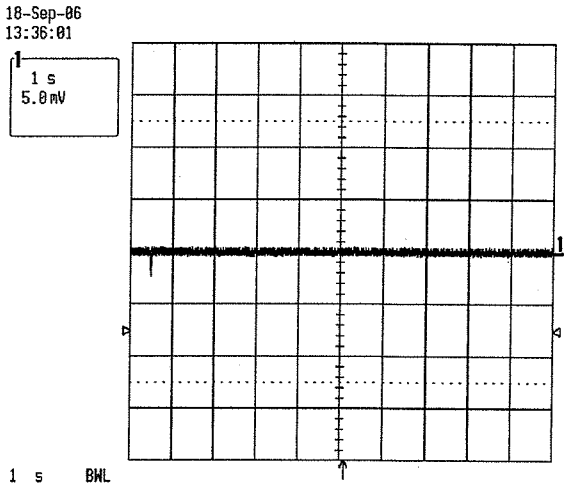

figure 1 An oscilloscope trace of the output of a 38 mm 9102B photomultiplier. Note only a single event of about 10 photoelectrons equivalent has been recorded in 10 seconds.

The measurement covers 10 seconds and there is only one event, of about 10 photoelectrons high. Contrast this with the trace for a large diameter photomultiplier with a thicker window, depicted in **figure 2**.

The oscilloscope setting is now 20 mV/cm, compared with 5 mV for the 38 mm photomultiplier of **figure 1**, and yet there are considerably more 5 mV events and even

some of about 50 mV (100 to 200 photoelectrons equivalent). The relevance of the diameter and the thickness of the window to the background contribution will become obvious later.

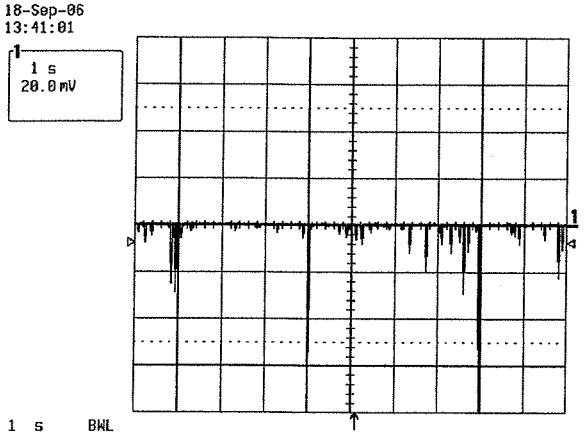

figure 2 The trace for a 5" 9390B operated at 5 x 10^5 gain. The oscilloscope sensitivity is 20 mV/cm and yet the number of pulses is considerably higher than those in Figure 1.

5 the photomultiplier background spectrum measured with a multichannel analyser

Dark count spectra were measured for a total of five photomultipliers. Two runs were necessary for each photomuliplier in order to cover the entire pulse height span from 0.1 to 1000 photoelectrons equivalent. Data for the low energy half of the spectrum required only an hour to accumulate sufficient data; whereas 12 hours was devoted to attaining results with good statistical precision for that part of the spectrum covering 5 to 1000 photoelectrons. The mean pulse height for single photoelectrons was determined by recording a pulse height distribution for each pmt. The scale in photoelectrons equivalent shown in **figure 3** for example is based on the mean pulse height for each pmt. Differential pulse height distributions are shown in **figures 3(a) to (d)** for photomulipliers fabricated with borosilicate windows; tube diameters range from 38 to 134 mm. The cosmic ray peak is clearly resolved in all the figures, except that for the 38 mm photomultiplier where only a shoulder at about 15 photoelectrons is observed. The 9390, in **figure 3(d)**, shows the muon peak at

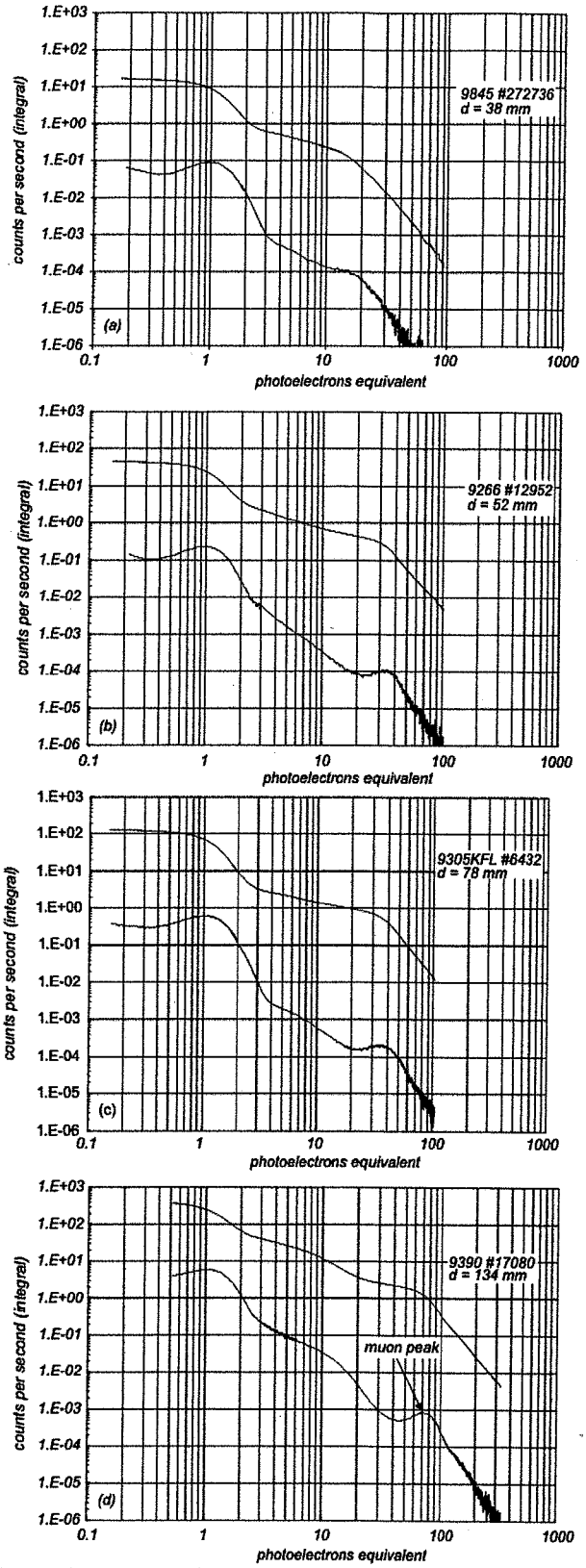

figure 3 (a) – (d) Differential and integral pulse height distributions measured for a set of photomultipliers of different window diameter, and different window thickness. Each differential curve shows a clearly resolved muon peak, except the 38 mm pmt. The integral distributions are particularly useful since they provide the expected number of counts above any stated photoelectron threshold.

80 photoelectrons. These four plots clearly support the proposition of a linear relationship between window thickness and the magnitude of the muon peak, measured in photoelectrons.

Light emission due to the Cerenkov effect is skewed towards the uv because the photon yield varies as $1/\lambda^2$. Borosilicate glass has a wavelength cut-off at about 300 nm, whereas the figure is 180 nm for quartz [6] - by cut-off we mean the wavelength at which transmission is reduced to 50%. The response of a quartz-windowed photomultiplier, shown in **Figure 4,** bears out the above arguments as we see that the photoelectron yield for a 9269QB is twice that from a 9305KB; both of these photomultiplier types have a similar window thickness.

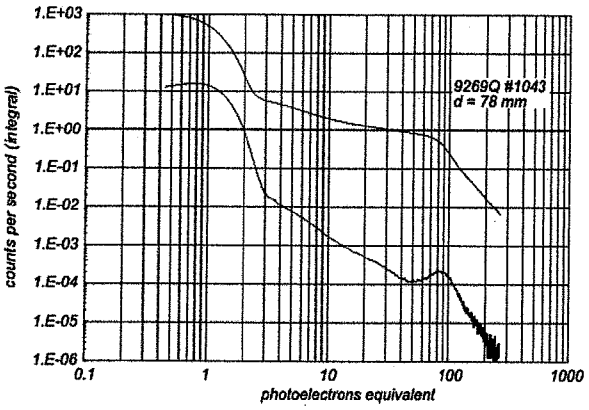

figure 4 Showing that the muon peak occurs at an even higher pulse height in a quartz pmt. The muon peak is clearly discernable at 85 photoelectrons equivalent compared with figure 3(c) above, where it occurs at 38 photoelectrons. Note the rate of the muon events, from the upper curve, is 1 per second, exactly the same as in figure 3(c), as it should be.

Table 2 The Cerenkov yield, y, in photoelectrons, pe, in photomultipliers, with different window thicknesses, t.

Type	d mm	t, mm	y(pe)	y(pe)/t mm^{-1}
9102B	38	1.43	~15	~9.8
9266B	51	2.41	32	13.2
9305KB	78	3.73	38	10.2
9390KB	134	6.38	74	11.6
9269QB	78	3.95	85	21.5

The rate of muons per cm^2 is readily deduced from any of the integral distributions. For the 3" pmt, for example, we have from **figure 3(c)**, that the integral rate is ~1.0 per second which equates to 1.0 x 60/47.7 = 1.25 /minute/cm^2, in agreement with the figure of 1.1 readily deduced from the data given in **Table 1**.

6 the effect of window orientation

The effect of pmt orientation was investigated in a third series of measurements. Three spectra were measured for the 9390KB 5" pmt, operated with the window: (a) pointing upwards; (b) pointing downwards and (c) vertical. These are shown in **figure 5(a) to (c).** We expect a higher yield, y, when the window points upwards compared with when it points downwards, although the number of muon events should not change. This is easily understood in terms of the angular dependence of the Cerenkov cone of emission (48° for glass), as shown in **figure 6(a)**. Cerenkov light is beamed forward in the same direction as the muon, much like a torch. Clearly when the window of the pmt is held vertical, the mean track length of the muons is increased over that for a horizontal orientation. There will, however, be fewer events, because of the smaller aperture presented to the muon flux through its $\cos^2\theta$ dependence. These are the arguments that Young [1] put forward and the results of **figure 4** clearly support his conclusions.

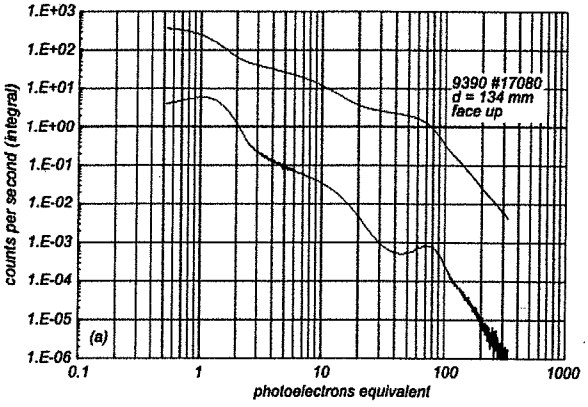

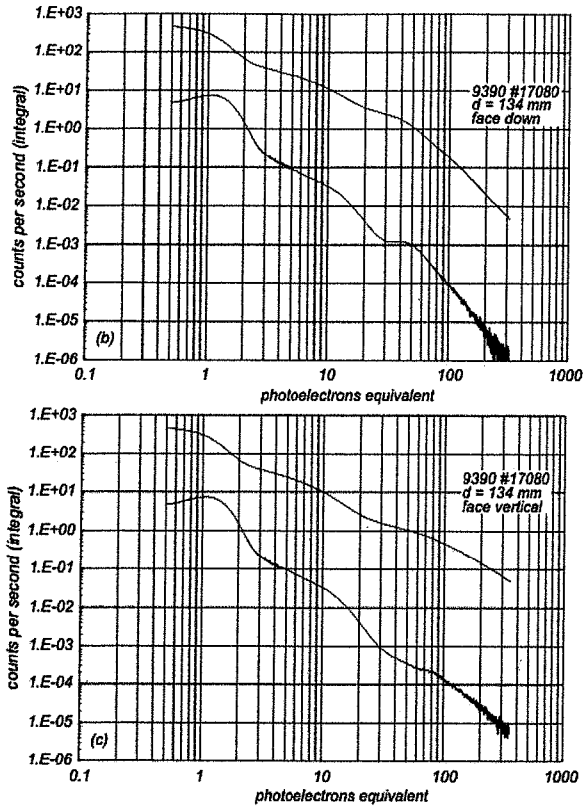

figure 5 Pulse height distributions for various orientations of the plane of the photomultiplier window. (a) the window faces upwards (b) the window faces downwards and (c) the window is vertical. Note in (c) that there are an order of magnitude more events > 300 pe equivalent than in the other two spectra.

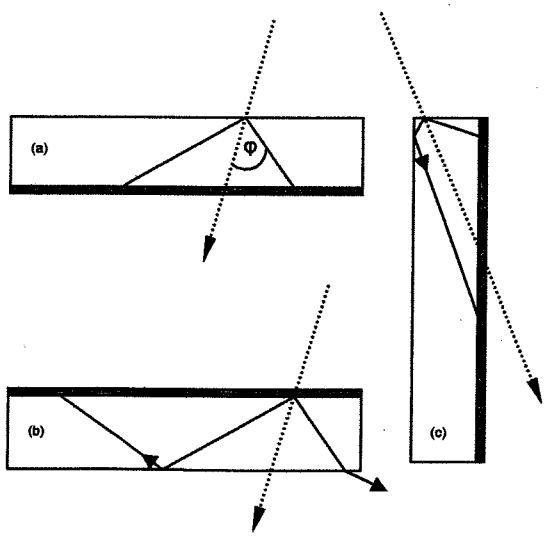

figure 6 Light emission by the Cerenkov effect. The cathode is indicated by the green tint and the dotted line represents the muon trajectory. It is clear that about half the light escapes the cathode in (b), compared with (a). Generation of large pulses is more likely in (c) than in the other orientations, although their frequency will be low.

7 the cosmic ray contribution in scintillation detectors

Cosmic ray muons afford a means of calibrating massive detectors found in astrophysics (Kamiokande, SNO, MACRO, Auger surface array and Borexino, for example) and in High Energy Physics experiments, such as LHC. Far from being a nuisance, these detectors have been calibrated in terms of MIPS (Minimum Ionizing Particles), which is exactly what a high energy muon is. Not only is the source of this calibration free, but it is readily available and constant. However, we will consider the effect of muons and the soft component on a NaI(Tl) detector of the type commonly used for radiation monitoring. **Figure 7** is a differential energy spectrum measured with a 1¼" by 1½" NaI(Tl) crystal mounted on the 38 mm diameter photomultiplier (with the window horizontal). The calibration is in terms of MeV rather than in photoelectrons; this was established using one of the peaks of a ^{60}Co radio-active source (1.17 and 1.33 MeV). There is a peak at 15 MeV from which we deduce that the muon signal in NaI(Tl) is ~5 MeV per cm of path length, consistent with an energy loss of 1.5 MeV/g. The energy range 0 to 5MeV was examined in greater detail revealing the spectrum of **figure 7(b).** This steeply falling part of the spectrum shows the well-known, naturally occurring, peaks of ^{214}Bi, ^{208}Tl and ^{40}K. The first two of which belong to the Uranium and Thorium decay schemes and the third is a long-lived isotope of potassium. Detailed information on this topic may be found in [7]. There are no discernable peaks beyond 2.6 MeV, which is where the cosmic ray contribution starts – initially, mainly the soft component, followed by the muon contribution.

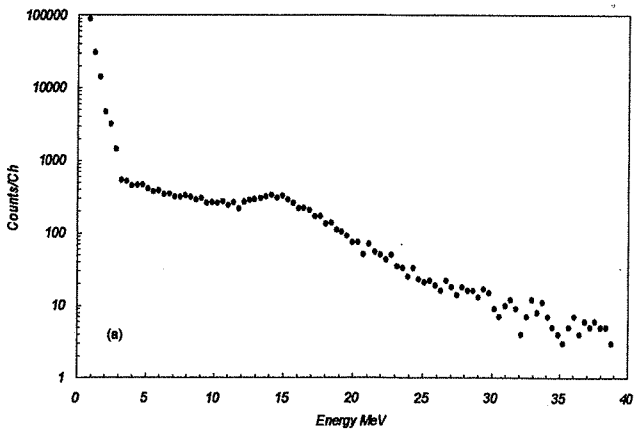

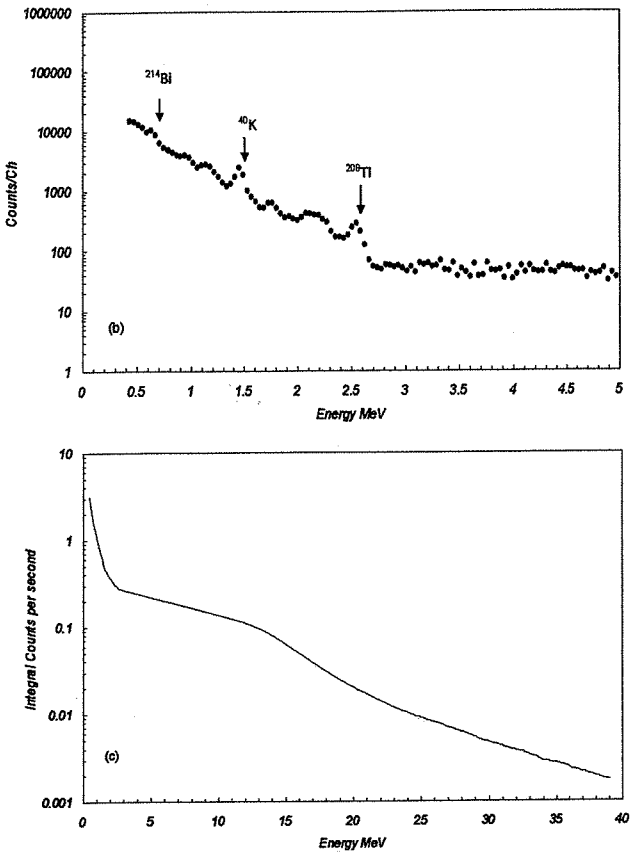

figure 7 Background spectrum measured with a 1¼" by 1½" NaI(Tl) crystal. Note the integral rate at ~ 0.1 per second agrees with the rate for the bare 38 mm pmt.

8 conclusions

Cosmic ray muons generate Cerenkov photons as they pass through the window of the photomultiplier. The typical size of the pulse, for borosilicate glass, is ~12 photoelectrons per mm of window traversed. The figure for fused silica (quartz) is ~twice this at 21.5 pe/mm of path length.

The rate of Cerenkov events is proportional to the area of the window and to some extent on its orientation. The rate deduced from the present measurements is ~1.25 cm^{-2} $minute^{-1}$, consistent with the well-established sea-level cosmic ray muon rate of 1.1 cm^{-2} $minute^{-1}$.

Some photomultiplier users have reported that certain pmts of the same type are worse than others regarding the number of spikes they produce. This cannot be explained in terms of glass tolerances and the answer is more likely to be found in pmt gain differences. The slope of the integral distribution beyond the muon peak, for example, is very steep and any attempt to quantify the number of big pulses observed will depend critically on the assumed gain setting. Setting the pmt consistently is particularly difficult in dc applications where reference to the SER is not possible. Muons also cause ionisation and excitation in the glass window and in the photocathode layer; a small number of muons will be accompanied by δ-rays, but all these contributions are small compared with the Cerenkov yield.

The group of photomultipliers used for measurement were selected to have similar spectral responses, with a typical peak QE of 25%. The results were, therefore, self-normalised.

references

[1] A T Young, Cosmic ray induced dark current in photomultipliers. Rev. Sci.Instrum., 37, number 11, 1472 – 81

[2] A E Sandstrom, Cosmic ray physics, North Holland Publishing Company, Amsterdam, 1965, p64.

[3] O C Allkofer and P K F Greider, Cosmic rays on earth, Energie Physik Mathematik GmbH, Karlsruhe, 1984

[4] A T Young, Photometric error analysis IX: Optimum use of photomultipliers Appl. Opt. 8 2341 – 47

[5] A G Wright, An investigation of photomultiplier background, J Phys. E, 1983,16, 300 - 7

[6] Understanding photomultipliers, figure 3, Electron Tubes Ltd, UK. Ref: upmt/01

[7] A G Wright, Effect of radioactivity in photomultipliers for sensitive instrumentation. Electron Tubes Ltd, Technical Reprint Series, R/P082.

talk to us about your application or choose a product from our literature:

photomultipliers, voltage dividers, signal processing modules, housings and power supplies

ET Enterprises Limited
45 Riverside Way
Uxbridge UB8 2YF
United Kingdom
tel: +44 (0) 1895 200880
fax: +44 (0) 1895 270873
e-mail: sales@et-enterprises.com
web site: www.et-enterprises.com

ADIT Electron Tubes
300 Crane Street
Sweetwater TX 79556 USA
tel: (325) 235 1418
toll free: (800) 521 8382
fax: (325) 235 2872
e-mail: sales@electrontubes.com
web site: www.electrontubes.com

choose accessories for this pmt on our website

an ISO 9001 registered company

ET Enterprises electron tubes

DS_ R/P100 Issue 3 (18/01/11)